Cell Death and Differentiation (2013) 20, 1161–1173

www.nature.com/cdd

Obatoclax (GX15-070) triggers necroptosis by promoting the assembly of the necrosome on autophagosomal membranes

F Basit[1], S Cristofanon[1] and S Fulda*[1]

Obatoclax (GX15-070), a small-molecule inhibitor of antiapoptotic Bcl-2 proteins, has been reported to trigger cell death via autophagy. However, the underlying molecular mechanisms have remained elusive. Here, we identify GX15-070-stimulated assembly of the necrosome on autophagosomal membranes as a key event that connects GX15-070-stimulated autophagy to necroptosis. GX15-070 predominately induces a non-apoptotic form of cell death in rhabdomyosarcoma cells, as evident by lack of typical apoptotic features such as DNA fragmentation or caspase activation and by insensitivity to the broad-range caspase inhibitor zVAD.fmk. Instead, GX15-070 triggers massive accumulation of autophagosomes, which are required for GX15-070-induced cell death, as blockade of autophagosome formation by silencing of Atg5 or Atg7 abolishes GX15-070-mediated cell death. Co-immunoprecipitation studies reveal that GX15-070 stimulates the interaction of Atg5, a constituent of autophagosomal membranes, with components of the necrosome such as FADD, RIP1 and RIP3. This GX15-070-induced assembly of the necrosome on autophagosomes occurs in a Atg5-dependent manner, as knockdown of Atg5 abrogates formation of this complex. RIP1 is necessary for GX15-070-induced cell death, as both genetic and pharmacological inhibition of RIP1 by shRNA-mediated knockdown or by the RIP1 inhibitor necrostatin-1 blocks GX15-070-induced cell death. Similarly, RIP3 knockdown rescues GX15-070-mediated cell death and suppression of clonogenic survival. Interestingly, RIP1 or RIP3 silencing has no effect on GX15-070-stimulated autophagosome formation, underlining that RIP1 and RIP3 mediate cell death downstream of autophagy induction. Of note, GX15-070 significantly suppresses tumor growth in a RIP1-dependent manner in the chorioallantoic membrane model *in vivo*. In conclusion, GX15-070 triggers necroptosis by promoting the assembly of the necrosome on autophagosomes. These findings provide novel insights into the molecular mechanisms of GX15-070-induced non-apoptotic cell death.
Cell Death and Differentiation (2013) **20,** 1161–1173; doi:10.1038/cdd.2013.45; published online 7 June 2013

Programmed cell death represents a basic cellular process that is frequently disturbed in human diseases.[1] There are several distinct forms of programmed cell death, including apoptosis, necroptosis and autophagic cell death.[2] Evasion of programmed cell death constitutes a hallmark of human cancers and may be caused by dysregulation of pro- and antiapoptotic signals.[3] For example, antiapoptotic proteins of the Bcl-2 family proteins are frequently overexpressed in human cancers.[4] As high expression levels of antiapoptotic Bcl-2 proteins can confer treatment resistance, small-molecule inhibitors have been developed to neutralize their cytoprotective functions.[5]

GX15-070 is a small-molecule indole bipyrrole compound that antagonizes Bcl-2, Bcl-X_L, Bcl-w and Mcl-1.[5] Although GX15-070 as single agent or in combination regimens is currently under clinical evaluation for the treatment of hematological malignancies and solid tumors,[6] the molecular mechanisms of its antitumor activity have still not been fully resolved. By neutralizing antiapoptotic Bcl-2 proteins, GX15-070 has been shown to engage the mitochondrial (intrinsic) pathways of apoptosis.[7–9] In addition to apoptosis, non-apoptotic cell death pathways, in particular autophagy, have been implicated in GX15-070-mediated cytotoxicity.[9–13]

Macroautophagy (hereafter referred to as autophagy) is an evolutionarily conserved, ubiquitous and multi-step process by which cytosolic material is sequestered in a double-layered membrane, delivered to the lysosome for degradation and recycled to fuel cellular growth.[14] Autophagy starts with the formation of an isolation membrane also called phagophore that elongates, encapsulates cytoplasmatic cargo and seals to form the autophagosome.[14] Vesicle elongation and formation of the autophagosome are cooperatively mediated by two ubiquitin-like conjugation systems. The Atg12 conjugation system involves the covalent conjugation of Atg12 to Atg5, which then interacts with Atg16L to form the Atg5-Atg12-Atg16L complex.[15] In the second pathway, phosphatidylethanolamine is conjugated to LC3, one of the mammalian homologues of Atg8, which leads to the

[1]Institute for Experimental Cancer Research in Pediatrics, Goethe-University, Komturstr. 3a, Frankfurt 60528, Germany
*Corresponding author: S Fulda, Institute for Experimental Cancer Research in Pediatrics, Goethe-University, Komturstr. 3a, Frankfurt 60528, Germany.
Tel: +49 69 67866557; Fax: +49 69 6786659157; E-mail: simone.fulda@kgu.de
Keywords: Obatoclax (GX15-070); necroptosis; autophagy; RIP1; rhabdomyosarcoma
Abbreviations: ERMS, embryonal rhabdomyosarcoma; ARMS, alveolar rhabdomyosarcoma; BafA1, Bafilomycin A1; Nec-1, necrostatin-1; CAM, chorioallantoic membrane; TNFα, tumor necrosis factor α; RIP, receptor-interacting protein; RMS, rhabdomyosarcoma; zVAD.fmk, N-benzyloxycarbonyl-Val-Ala-Asp-fluoromethylketone
Received 23.12.12; revised 04.4.13; accepted 05.4.13; Edited by G Kroemer; published online 07.6.2013

conversion of the soluble form of LC, that is, LC3-I, to the autophagic-vesicle-associated form LC3-II.[15] The autophagosome eventually fuses with the lysosome to generate the autophagolysosome where the cargo is broken down into its constituent components.[14] Autophagy is often engaged as part of a cellular stress reaction upon exposure to cytotoxic drugs and can exert dual functions in the regulation of either cell death or survival, likely in a context-dependent manner.[16]

Although GX15-070 has been shown to engage autophagy,[9,10,17–19] possibly via the disruption of the Beclin1/Mcl-1 interaction,[10,11] the critical question whether or not GX15-070-stimulated autophagic activity promotes or inhibits cell death has been controversially discussed. On one side, GX15-070-induced autophagy has been linked to cell death, as genetic or pharmacological blockage of autophagy was found to inhibit cell death.[9–11] On the other side, inhibition of autophagy was described to enhance GX15-070-induced cell death, supporting a cytoprotective function of autophagy.[18] Besides this controversial discussion on the functional relevance of autophagy for GX15-070-triggered cytotoxicity, the molecular mechanisms of autophagic cell death upon treatment with GX15-070 have remained elusive.

Necroptosis (programmed necrosis) represents another regulated, caspase-independent mode of cell death.[2] The serine/threonine kinases receptor-interacting protein 1 (RIP1) and RIP3 are critical components of the necrosome, a cytosolic multiprotein complex that is required for necroptosis signaling.[20] RIP1 has been identified in a genome-wide screen as a key regulator of necroptosis[21] and its kinase activity was shown to be necessary for the induction of necroptosis by phosphorylating RIP3.[22] In addition to tumor necrosis factor α (TNFα)-mediated necroptotic cell death,[23] necroptosis can be initiated by several cellular stress stimuli, including DNA damage, ROS species and hypoxia.[23]

Rhabdomyosarcoma (RMS) is the most frequent pediatric soft tissue sarcoma and can be classified into two major pathological subtypes, that is, embryonal RMS (ERMS) and alveolar RMS (ARMS).[24] ARMS frequently harbors reciprocal chromosomal translocations between chromosomes 1 or 2 and chromosome 13, resulting in chimeric fusion genes composed of PAX3 or PAX7 and FOXO1A.[25] Both PAX3 and PAX3/FKHR transcription factors were reported to stimulate Bcl-X_L mRNA expression in RMS.[26] In addition, Mcl-1 was found to be frequently overexpressed in RMS,[27] supporting the notion that Bcl-2 proteins are dysregulated in RMS.[28] The prognosis for children with RMS is still poor irrespective of aggressive multimodal treatment protocols,[29] underscoring the need for innovative therapeutic approaches. In the present study, we used RMS as a model to investigate the molecular mechanisms of GX15-070-induced cytotoxicity.

Results

GX15-070 induces non-apoptotic, caspase-independent cell death in RMS cells. Initially, we examined the expression levels of key pro- and antiapoptotic Bcl-2 proteins in several RMS cell lines, which represent ERMS (RD, TE671) and ARMS (RMS13, Rh30, Rh41). RMS cell lines expressed the antiapoptotic Bcl-2 proteins Bcl-2, Bcl-X_L and Mcl-1, the multidomain proapoptotic Bcl-2 proteins Bax and Bak and the BH3-only proteins Bid, Bim and Noxa (Figure 1a).

Next, we investigated the responsiveness of RMS cell lines to GX15-070. Treatment with GX15-070 reduced cell viability in a dose-dependent manner in all RMS cell lines at nanomolar concentrations (Figure 1b). As TE671 and RMS13 cells turned out to be most responsive to GX15-070 and as they represent the two major subtypes of RMS, that is, ERMS and ARMS, we selected these two cell lines for further mechanistic studies. Kinetic analysis showed that GX15-070 decreased cell viability in a time-dependent manner (Figure 1c).

To investigate whether cells die via apoptosis, we analyzed DNA fragmentation, a characteristic feature of apoptotic cell death. We noticed that GX15-070 caused little DNA fragmentation under conditions where the majority of cells already lost their viability, for example, upon treatment with 200 nM GX15-070 for 48 h (Figures 1c and d). By comparison, treatment with ABT-737, a small-molecule inhibitor of Bcl-2, Bcl-X_L and Bcl-w that was used as a positive control to induce apoptosis, triggered loss of cell viability in parallel with massive DNA fragmentation (Supplementary Figure S1). In addition, GX15-070-treated cells displayed swollen cytoplasm but lacked typical apoptotic features such as plasma membrane blebbing and nuclear fragmentation, which were observed in ABT-737-treated cells (Supplementary Figure S2), further pointing to a non-apoptotic mode of cell death by GX15-070.

To explore whether GX15-070-induced cell death depends on caspase activity, we examined the effect of the broad-spectrum caspase inhibitor N-benzyloxycarbonyl-Val-Ala-Asp-fluoromethylketone (zVAD.fmk). Of note, zVAD.fmk failed to block both loss of cell viability as well as DNA fragmentation upon treatment with GX15-070 (Figures 2a and b), whereas it almost completely rescued cell viability as well as DNA fragmentation in response to ABT-737 that was used as positive control for inducing apoptosis (Supplementary Figure S3). Consistently, monitoring activation of the caspase cascade by western blot analysis revealed little cleavage of caspase-8, -9 or -3 by GX15-070, whereas ABT-737 triggered cleavage of caspases into active fragments (Figure 2c). Furthermore, neither knockdown nor overexpression of Bcl-2 substantially altered GX15-070-induced cell death (Supplementary Figure S4).

Furthermore, we examined whether GX15-070-induced cell death depends on autocrine/paracrine TNFα signaling using both a pharmacological and a genetic approach. Addition of the TNFα-blocking antibody Enbrel failed to rescue GX15-070-induced cell death, whereas Enbrel significantly protected against cell death following treatment with TNFα and IAP inhibitor 3 used as a positive control (Figures 2d and e). Similarly, RNA interference-mediated knockdown of TNFR1 did not prevent GX15-070-induced cell death (Figures 2f–h). Together, this set of experiments indicates that GX15-070 predominately induces a non-apoptotic, caspase- and TNFα-independent form of cell death.

GX15-070 induces autophagy. As autophagy has been implicated in caspase-independent cell death triggered by GX15-070,[9–12] we next asked whether GX15-070 stimulates autophagy in RMS cells. Indeed, GX15-070 triggered

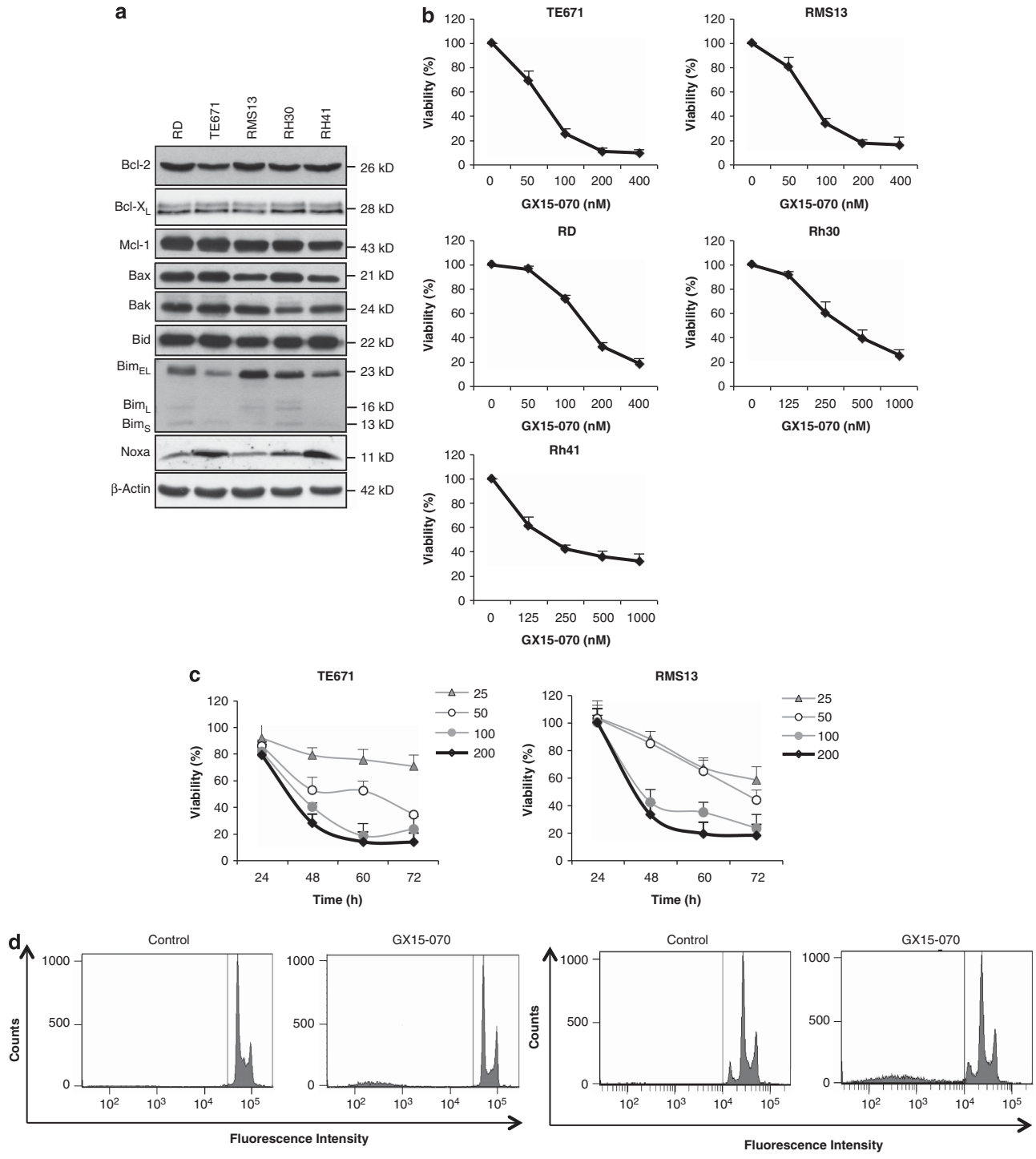

Figure 1 GX15-070-induced cell death in RMS cells. (**a**) Expression levels of anti- and proapoptotic Bcl-2 family proteins in RMS cells were assessed by western blot analysis. β-Actin was used as loading control. (**b** and **c**) RMS cells were treated with the indicated concentrations of GX15-070 for 72 h (**b**) or with the indicated concentrations of GX15-070 for the indicated times (**c**). Cell viability was determined by MTT assay and is expressed as percentage of untreated controls. Data represent mean + S.D. of three independent experiments performed in triplicate. (**d**) TE671 and RMS13 cells were treated with 200 nM GX15-070 for 48 h. Apoptosis was determined by fluorescence-activated cell-sorting analysis of DNA fragmentation of propidium iodide-stained nuclei. Representative histograms of three independent experiments are shown

massive conversion of LC3-I to LC3-II (Figure 3a). To distinguish whether this accumulation of autophagosomes is caused by increased production or, alternatively, by reduced clearance due to disruption of the autophagic flux, we examined GX15-070-stimulated autophagosome formation in the presence and absence of Bafilomycin A1 (BafA1). BafA1 is a specific inhibitor of the lysosomal proton pump that disrupts the autophagic flux by preventing the fusion of autophagosomes with lysosomes.[30] We detected increased LC3-II levels after cotreatment with GX15-070 and

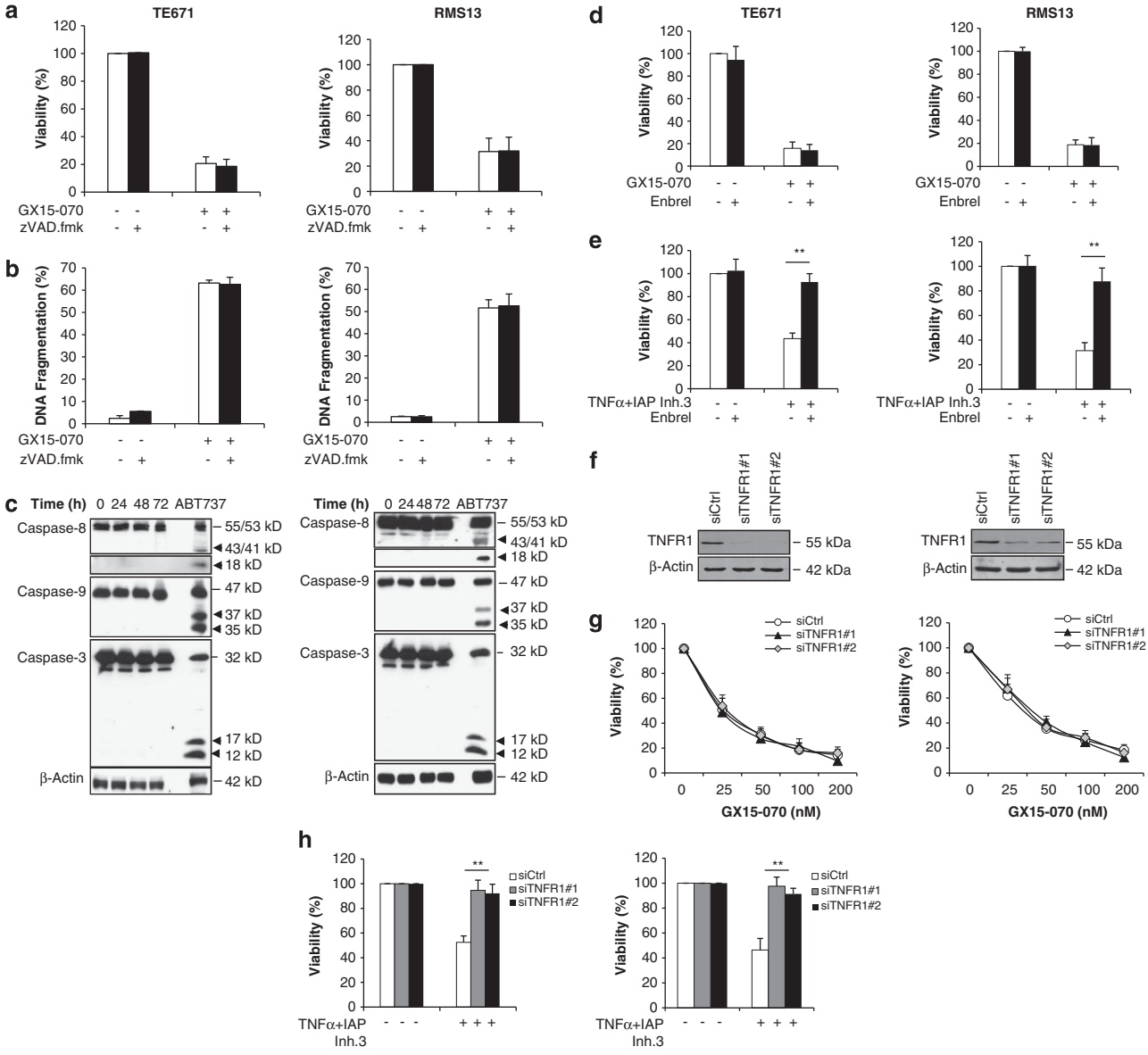

Figure 2 GX15-070 triggers caspase-independent cell death in RMS cells. (**a** and **b**) TE671 and RMS13 cells were treated for 72 h with 200 nM GX15-070 in the presence or absence of 20 μM zVAD.fmk. Cell viability was determined by MTT assay and is expressed as percentage of untreated controls (**a**). Apoptosis was determined by fluorescence-activated cell-sorting analysis of DNA fragmentation of propidium iodide-stained nuclei (**b**). Data represent mean + S.D. of three independent experiments performed in triplicate. (**c**) TE671 and RMS13 cells were treated with 200 nM GX15-070 for the indicated time points or with 10 μM ABT-737 for 3 h. Caspase activation was assessed by western blotting. Arrowheads indicate caspase cleavage fragments. (**d** and **e**) TE671 and RMS13 cells were treated for 72 h with 200 nM GX15-070 (**d**) or 100 ng/ml TNFα and 10 μM IAP (inhibitor of apoptosis) inhibitor 3 (**e**) in the presence or absence of 20 μg/ml Enbrel. Cell viability was determined by MTT assay and is expressed as percentage of untreated controls. (**f**–**h**) TE671 and RMS13 cells were transfected with control siRNA (siCtrl) or two distinct siRNA sequences against TNFR1 (siTNFR1#1, siTNFR1#2). Expression of TNFR1 was determined by western blotting (**f**) Cell viability was determined by MTT assay after treatment for 72 h with the indicated concentrations of GX15-070 (**g**) or with 100 ng/ml TNFα and 10 μM IAP inhibitor 3 (**h**) and is expressed as percentage of untreated controls. In panels **a**, **b**, **d**, **e**, **g** and **h**, data represent mean + S.D. of three independent experiments performed in triplicate; $^{**}P < 0.001$

BafA1 compared with treatment with GX15-070 or BafA1 alone (Figure 3b), suggesting that GX15-070 does not primarily disrupt the autophagic flux. In addition, we monitored the autophagic flux by using a tandem mCherry-GFP-tagged LC3 construct. As the GFP signal is acid-sensitive and the mCherry-tag is acid-insensitive, autophagosomes emit yellow fluorescence derived from both tags, while autophagolysosomes exhibit red fluorescence, as the green GFP-tag is degraded upon fusion of autophagosomes with lysosomes. We found that treatment with GX15-070 triggered the formation of red dots indicative of an ongoing autophagic flux where autophagosomes fuse with lysosomes (Figure 3c). By contrast, treatment with BafA1 increased the number of yellow dots consistent with the disruption of the autophagic flux by BafA1 (Figure 3c). Cotreatment with GX15-070 and BafA1 yielded both red and

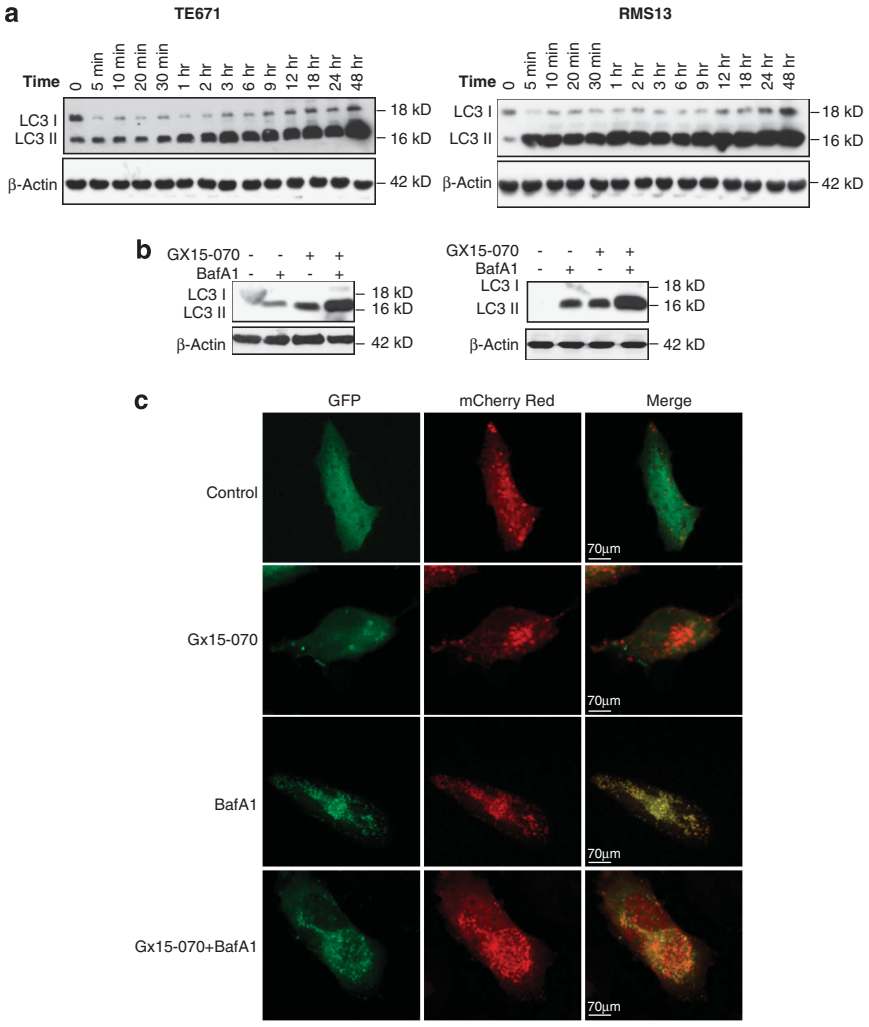

Figure 3 GX15-070 induces autophagy in RMS cells. (**a** and **b**) TE671 and RMS13 cells were treated with 200 nM GX15-070 for the indicated time points (**a**) or with 200 nM GX15-070 for 3 h in the presence or absence of 1 μM BafA1 (**b**). LC3 lipidation was assessed by western blotting. (**c**) TE671 cells were transfected with tandem mCherry-GFP-tagged LC3 and were treated with 200 nM GX15-070 for 3 h in the presence or absence of 1 μM BafA1. Fluorescence of LC3 was detected by confocal microscopy

yellow dots (Figure 3c). These findings indicate that GX15-070 stimulates autophagy by increasing the production of autophagosomes rather than blocking the autophagic flux.

Atg5 and Atg7 are required for GX15-070-induced autophagy and cell death. As autophagy can exert either cytoprotective or cytotoxic functions depending on the context, we next asked whether autophagy inhibits or promotes GX15-070-mediated cell death. To address this question, we silenced Atg5 to block the induction of autophagy by GX15-070. Efficient knockdown of Atg5 protein by two distinct shRNA vectors was confirmed by western blot analysis compared with the control vector harboring a non-silencing sequence (Figure 4a). Silencing of Atg5 profoundly impaired the conversion of LC3-I to LC3-II upon treatment with GX15-070, demonstrating that it inhibits autophagosome formation (Figure 4b). Importantly, Atg5 knockdown significantly rescued GX15-070-triggered loss of cell viability compared with cells harboring the control vector (Figure 4c).

To further test the requirement of autophagy in GX15-070-induced cell death, we used a second approach to interfere with autophagosome formation by RNAi-mediated knockdown of Atg7. Control experiments showed that silencing of Atg7 caused efficient knockdown of Atg7 protein compared with a non-silencing control siRNA sequence (Figure 4d) and markedly inhibited GX15-070-stimulated conversion of LC3-I to LC3-II (Figure 4e). Similar to Atg5, also knockdown of Atg7 significantly reduced loss of cell viability upon GX15-070 treatment (Figure 4f), thus confirming that induction of autophagy is required for GX15-070-stimulated cell death.

GX15-070 triggers the assembly of the necrosome on autophagosomes. Having established that autophagy is necessary for GX15-070-mediated cytotoxicity, we next aimed at understanding how the autophagic machinery is connected to cell death signaling pathways. To this end, we asked whether GX15-070-triggered formation of autophagosomal membranes may serve as a cytosolic signaling

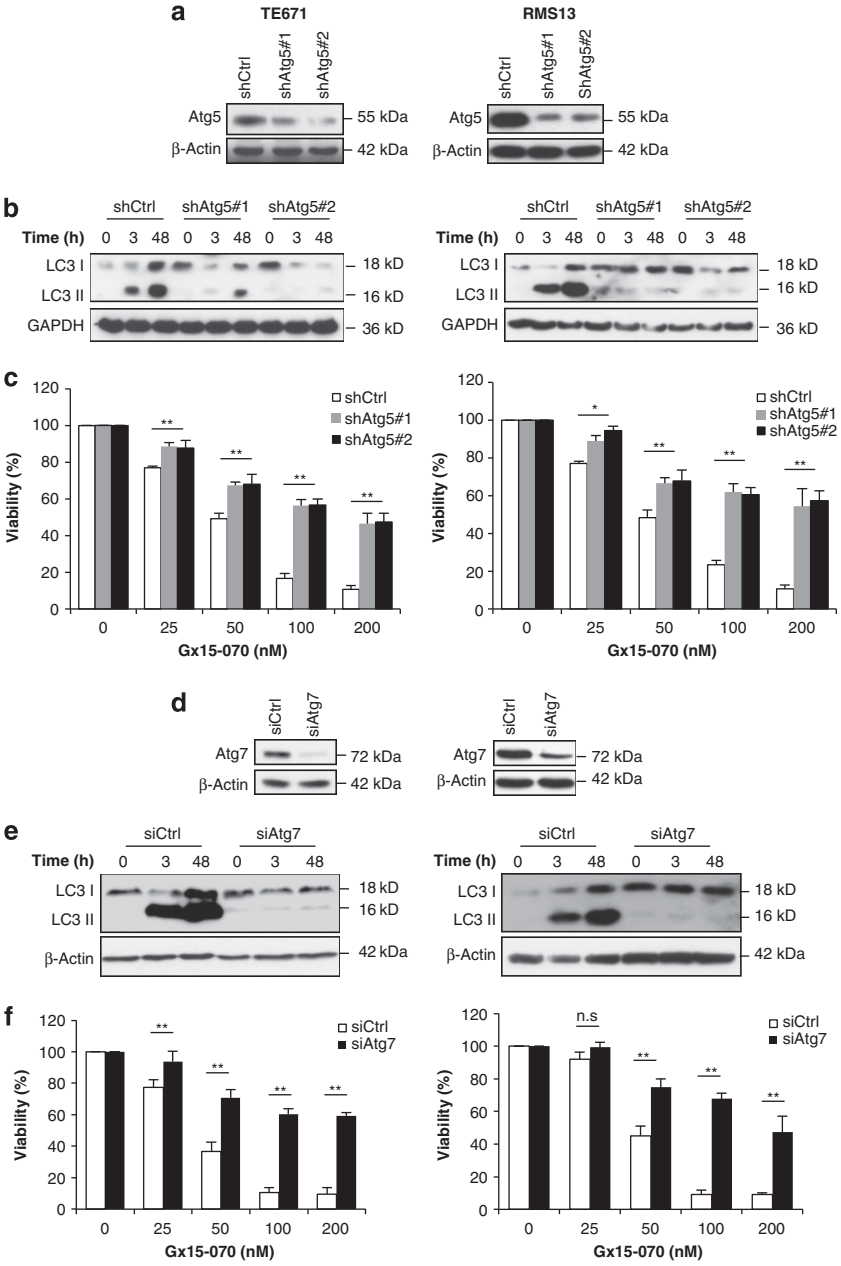

Figure 4 Atg5 and Atg7 are required for GX15-070-induced autophagy and cell death. (**a**) TE671 and RMS13 cells were transduced with control vector (shCtrl) or vectors containing two distinct shRNA sequences against Atg5 (shAtg5#1, shAtg5#2). Expression of Atg5 was determined by western blotting. (**b**) TE671 and RMS13 cells were treated with 100 nM GX15-070 for the indicated time points and LC3 lipidation was assessed by western blotting. (**c**) TE671 and RMS13 cells were treated with the indicated concentrations of GX15-070 for 72 h. Cell viability was determined by MTT assay and is expressed as percentage of untreated controls. Data represent mean + S.D. of three independent experiments performed in triplicate; $*P<0.05$; $**P<0.001$ comparing control with Atg5 knockdown cells. (**d**) TE671 and RMS13 cells were transfected with control siRNA (siCtrl) or siRNA targeting Atg7 (siAtg7). Expression of RIP1 was determined by western blotting. (**e**) TE671 and RMS13 cells were treated with 100 nM GX15-070 for the indicated time points and LC3 lipidation was detected by western blotting. (**f**) TE671 and RMS13 cells were treated with the indicated concentrations of GX15-070 for 72 h. Cell viability was determined by MTT assay and is expressed as percentage of untreated controls. Data represent mean + S.D. of three independent experiments performed in triplicate; $*P<0.05$; $**P<0.001$ comparing control with Atg7 knockdown cells

platform to initiate cell death. To address this question, we immunoprecipitated RIP1 as a key signaling molecule and analyzed its interaction partners. Interestingly, GX15-070 stimulated the interaction of Atg5, a constituent of autophagosomal membranes, with FADD, RIP1 and RIP3, which are components of the necrosome (Figure 5a). By comparison, caspase-8 was not detected in this complex, although caspase-8 protein was expressed in whole-cell lysates (Figure 5a). These findings indicate that GX15-070 triggers the recruitment of the necrosome to autophagosomal membranes.

To investigate whether the formation of this Atg5/FADD/RIP1/RIP3 complex indeed depends on the presence of autophagosomal membranes, we compared the assembly of

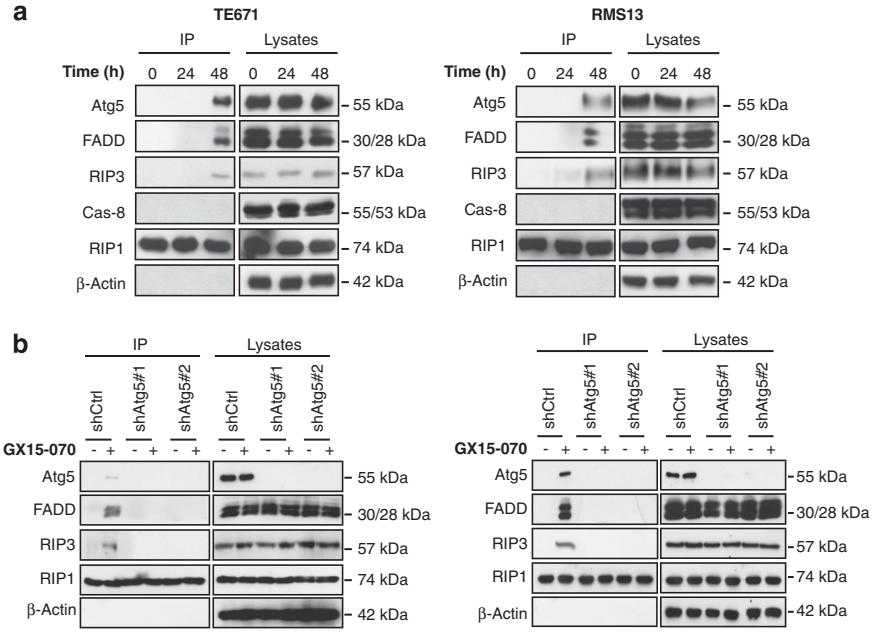

Figure 5 GX15-070 triggers the assembly of the necrosome on autophagosomes. (**a**) TE671 and RMS13 cells were treated with 200 nM GX15-070 for the indicated time points. RIP1 was immunoprecipitated (IP) using anti-RIP1 antibody. Atg5, FADD, RIP3 and caspase-8 were detected by western blotting. (**b**) TE671 and RMS13 cells were transduced with control vector (shCtrl) or vectors containing two distinct shRNA sequences against Atg5 (shAtg5#1, shAtg5#2) and treated with 100 nM GX15-070 for 48 h. RIP1 was immunoprecipitated (IP) using anti-RIP1 antibody. Atg5, FADD, RIP3 and caspase-8 were detected by western blotting

this complex in Atg5 knockdown and control cells, which are deficient and proficient, respectively, in the generation of autophagosomes (Figure 4b). Strikingly, the interaction of RIP1 with FADD and RIP3 was completely abolished in Atg5 knockdown cells (Figure 5b), which were also severely impaired to produce autophagosomes (Figure 4b). This indicates that Atg5-mediated formation of autophagosomes is required for the assembly of the RIP1-, RIP3- and FADD-containing necrosome complex during GX15-070-induced cell death.

RIP1 and RIP3 are required for GX15-070-induced cell death downstream of autophagosome formation. Based on our findings that GX15-070 triggers the formation of the necrosome on autophagosomal membranes (Figure 5a), we then asked whether GX15-070 induces cell death by engaging necroptosis, a RIP1- and/or RIP3-dependent regulated necrosis.[2] To address this question, we used necrostatin-1 (Nec-1), a RIP1-specific inhibitor that has been reported to block necroptosis.[31] Of note, Nec-1 significantly rescued GX15-070-induced loss of cell viability (Figure 6a), demonstrating that RIP1 kinase activity is required for GX15-070-triggered cell death.

In addition to this pharmacological approach, we also used a genetic strategy to selectively silence RIP1 in order to test the requirement of necroptosis in GX15-070-triggered cell death. Control experiments confirmed efficient, shRNA-mediated knockdown of RIP1 protein (Figure 6b). Importantly, RIP1 silencing significantly rescued GX15-070-induced loss of cell viability (Figure 6c). To explore whether RIP1 knockdown has an impact also on long-term clonogenic survival in addition to supporting cell viability in short-term assays, we performed colony assays. Notably, RIP1 silencing significantly protected against GX15-070-induced suppression of clonogenic survival (Figure 6d).

To investigate whether RIP1 is required for the formation of the Atg5/FADD/RIP1/RIP3 complex, we examined complex formation in RIP1 knockdown and control cells by immunoprecipitating FADD. Importantly, the interaction of Atg5 and FADD with RIP3 was completely abolished in RIP1 knockdown cells (Figure 6e). This indicates that RIP1 is required for the formation of the necrosome complex on autophagosomes during GX15-070-induced cell death.

To further provide evidence that the induction of autophagosomes occurs before the assembly of the necrosome, we analyzed LC3 conversion in RIP1 knockdown and control cells. Interestingly, knockdown of RIP1 did not alter the conversion of LC3-I to LC3-II upon GX15-070 treatment (Figure 6f), thus placing GX15-070-stimulated autophagosome formation upstream of RIP1.

In addition to silencing RIP1, we also knocked down RIP3 to test the requirement of the necrosome for GX15-070-triggered cell death. Efficient silencing of RIP3 by shRNA vectors was confirmed by western blot analysis (Figure 7a). Importantly, RIP3 knockdown significantly inhibited loss of cell viability and considerably increased colony formation upon GX15-070 treatment compared with control vector cells (Figures 7b and c). Similar to RIP1, knockdown of RIP3 did not prevent GX15-070-stimulated conversion of LC3-I to LC3-II (Figure 7d).

This set of experiments demonstrates that both RIP1 and RIP3 are required for GX15-070-triggered cell death and suppression of long-term clonogenic survival downstream of autophagosome formation.

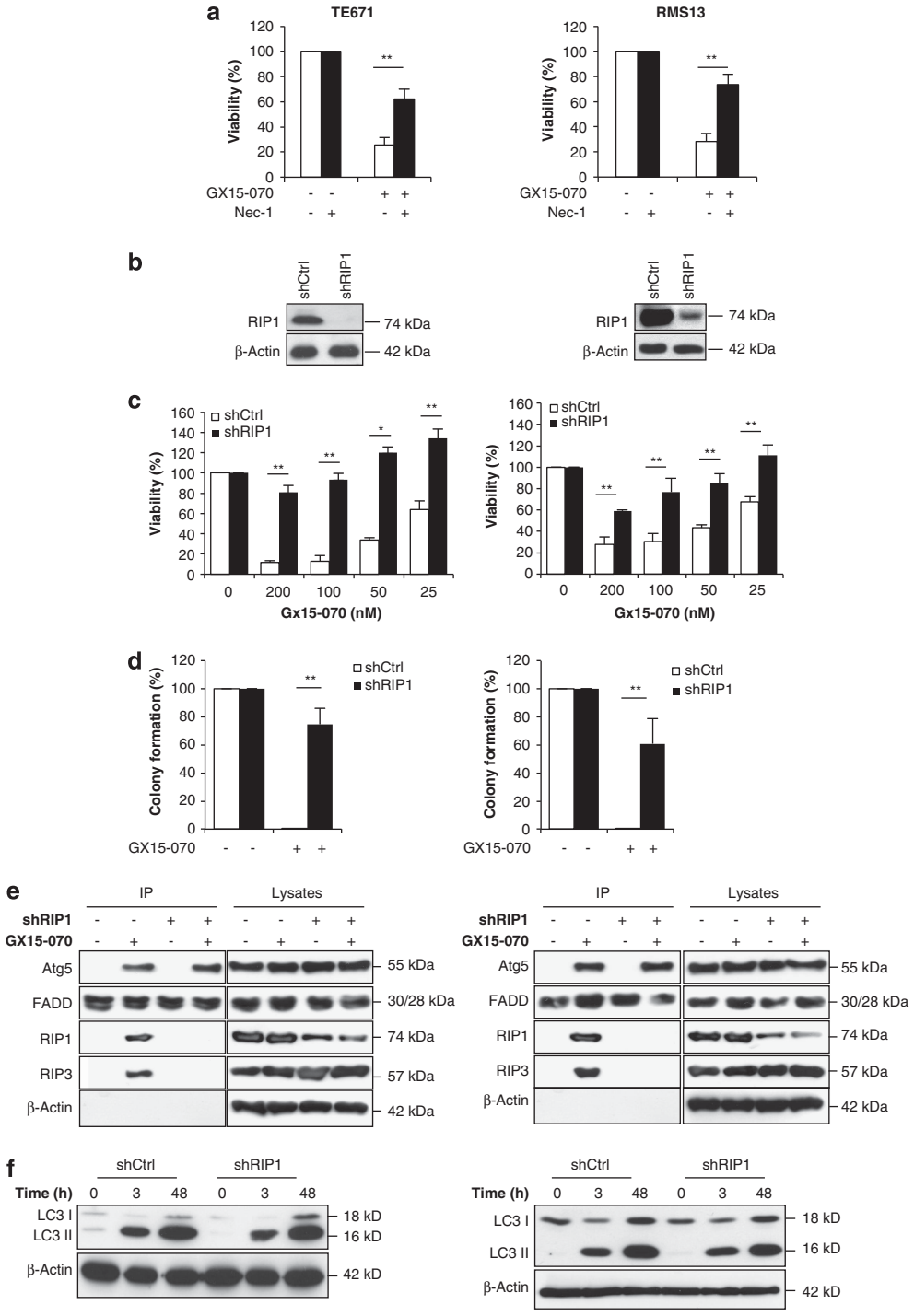

Figure 6 RIP1 is required for GX15-070-induced cell death downstream of autophagosome formation. (**a**) TE671 and RMS13 cells were treated with 200 nM GX15-070 in the presence or absence of 40 μg/ml Nec-1. Cell viability was determined by MTT assay and is expressed as percentage of untreated controls. (**b**) TE671 and RMS13 cells were transduced with control vector (shCtrl) and vector containing shRNA sequence against RIP1 (shRIP1). Expression of RIP1 was determined by western blotting. (**c**) TE671 and RMS13 cells were treated with the indicated concentrations of GX15-070 for 72 h. Cell viability was determined by MTT assay and is expressed as percentage of untreated controls. (**d**) TE671 and RMS13 cells were treated with 100 nM GX15-070 for 72 h before medium was exchanged by fresh drug-free medium. Colonies were stained with crystal violet and counted under the microscope. The percentage of colony numbers in the presence and absence of GX15-070 is shown. (**e**) TE671 and RMS13 cells were treated with 100 nM GX15-070 for 48 h. FADD was immunoprecipitated (IP) using anti-FADD antibody. Atg5, FADD, RIP1 and RIP3 were detected by western blotting. (**f**) TE671 and RMS13 cells were treated with 100 nM GX15-070 for the indicated time points and LC3 lipidation was detected by western blotting. In panels **a**, **c** and **d**, data represent mean + S.D. of three independent experiments performed in triplicate; $^{*}P<0.05$; $^{**}P<0.001$ comparing control with RIP1 knockdown cells (**c** and **d**) or cells treated in the presence and absence of Nec-1 (**a**)

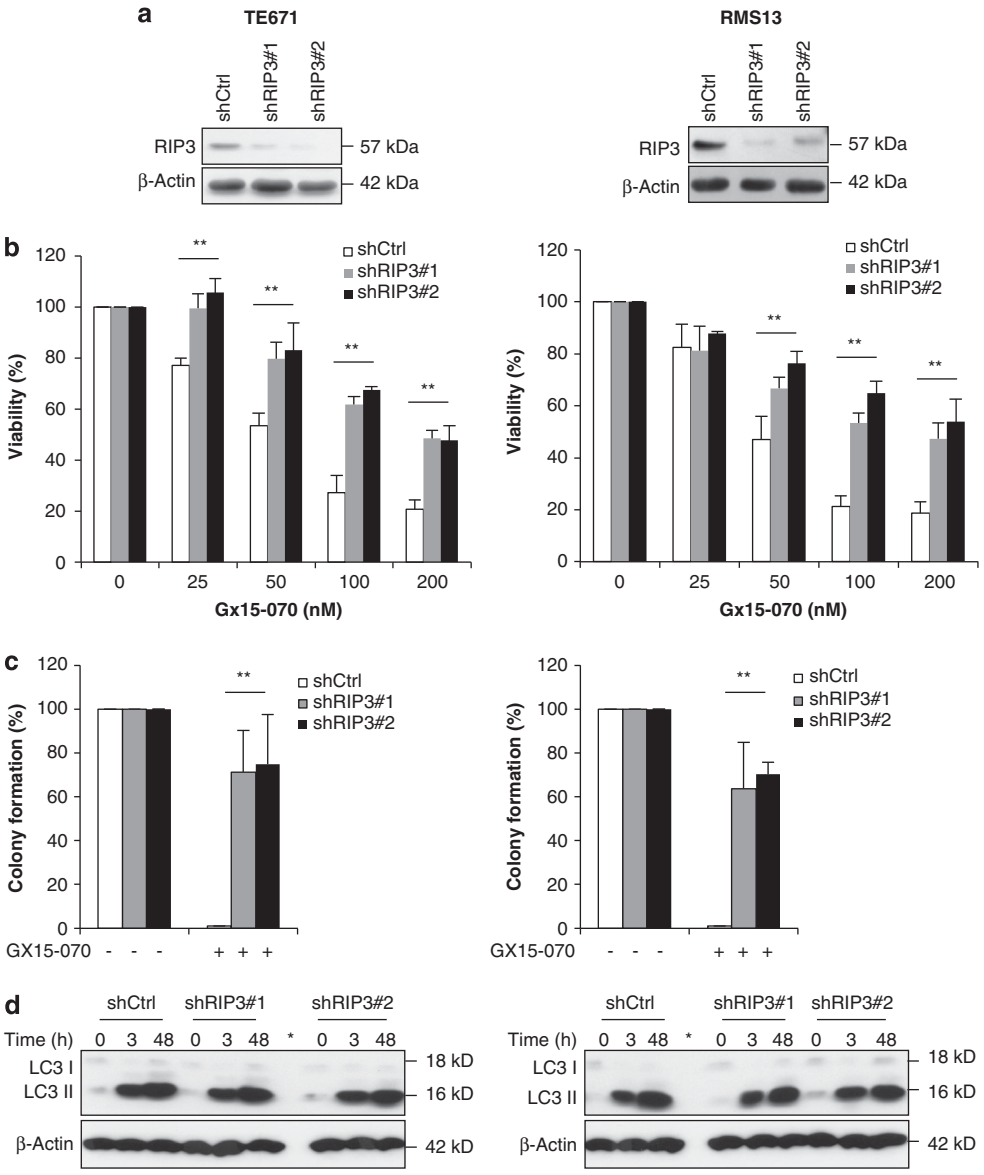

Figure 7 RIP3 is required for GX15-070-induced cell death downstream of autophagosome formation. (**a**) TE671 and RMS13 cells were transduced with control vector (shCtrl) and vectors containing shRNA sequences against RIP3 (shRIP3#1, shRIP3#2). Expression of RIP3 was determined by western blotting. (**b**) TE671 and RMS13 cells were treated with the indicated concentrations of GX15-070 for 72 h. Cell viability was determined by MTT assay and is expressed as percentage of untreated controls. (**c**) TE671 and RMS13 cells were treated with 100 nM GX15-070 for 72 h before medium was exchanged by fresh drug-free medium. Colonies were stained with crystal violet and counted under the microscope. The percentage of colony numbers in the presence and absence of GX15-070 is shown. (**d**) TE671 and RMS13 cells were treated with 100 nM GX15-070 for the indicated time points and LC3 lipidation was detected by western blotting; *indicates empty space between samples. In panels **b** and **c**, data represent mean + S.D. of three independent experiments performed in triplicate; $^{*}P<0.05$; $^{**}P<0.001$ comparing control with RIP3 knockdown cells

GX15-070 suppresses RMS growth *in vivo* in a RIP1-dependent manner. Finally, we evaluated the antitumor activity of GX15-070 and the requirement of RIP1 *in vivo* using the chicken chorioallantoic membrane (CAM) model, an established preclinical tumor model.[32,33] RMS cells were seeded on the CAM of chicken embryos and allowed to form tumors before treatment with GX15-070 was started. Importantly, treatment with GX15-070 significantly suppressed tumor growth of RMS *in vivo* (Figure 8). Of note, RIP1 knockdown significantly rescued this GX15-070-mediated suppression of tumor growth (Figure 8), indicating that RIP1 is required for the antitumor activity of GX15-070 *in vivo*.

Discussion

Although autophagy has previously been implicated in GX15-070-mediated cytotoxicity, the key question whether or not autophagy promotes or inhibits cell death in this context has been a subject of controversial discussion. Also, the biochemical events that link autophagy to cell death induction upon treatment with GX15-070 have so far remained elusive.

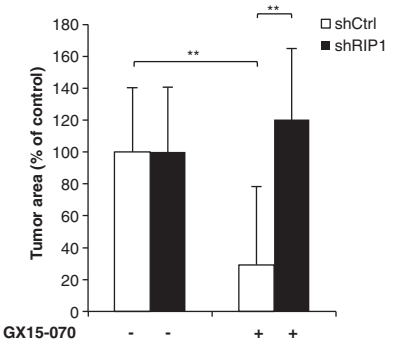

Figure 8 GX15-070 suppresses RMS growth *in vivo* in a RIP1-dependent manner. TE671 cells transduced with shRNA vectors against RIP1 or control shRNA were seeded on the CAM of chicken embryos and treated with 100 μM GX15-070 for 4 days. Tumor growth was analyzed using hematoxylin/eosin-stained paraffin sections of the CAM as described in Materials and Methods. Tumor area as percentage of the untreated control group is shown. Data represent mean + S.D. of 14 samples per group; $^{**}P < 0.001$

Here, we identify GX15-070-stimulated assembly of the necrosome on autophagosomal membranes as a key event that connects the induction of autophagy to cell death via necroptosis. GX15-070 causes massive accumulation of autophagosomes and promotes the interaction of Atg5, a component of autophagosomal membranes, with key constituents of the necrosome, that is, FADD, RIP1 and RIP3 (Supplementary Figure S5). This leads to the formation of a cytosolic cell death signaling complex that initiates necroptotic cell death. Several independent pieces of evidence support this conclusion.

First, GX15-070 triggers the assembly of large numbers of autophagosomes as demonstrated by massive conversion of LC3-I to LC3-II. Autophagic flux studies indicate that autophagy is predominately engaged by increased generation of autophagosomal membranes rather than disruption of the autophagic flux. GX15-070 has previously been shown to initiate autophagy by disrupting the interaction between Beclin1 and antiapoptotic Bcl-2 proteins, such as Mcl-1.[10,11] Second, this engagement of autophagy is required for GX15-070-induced cell death, as genetic silencing of autophagy genes such as Atg5 or Atg7 inhibits GX15-070-triggered accumulation of autophagosomal membranes as well as cell death. Third, RIP1 is necessary for GX15-070-induced cell death, as both genetic and pharmacological inhibition of RIP1 by RIP1 knockdown or by the RIP1-specific inhibitor Nec-1 blocks GX15-070-induced cell death. Fourth, similar to RIP1, genetic silencing of RIP3 rescues the GX15-070-induced cell death and suppression of clonogenic survival. Both RIP1 and RIP3 mediate cell death downstream of autophagy induction, as their knockdown inhibits GX15-070-induced cell death but not autophagosome formation. Thus, by dissecting the different steps of the signaling cascade during GX15-070-triggered cell death via selective knockdown or pharmacological inhibition of individual signaling components, we provide genetic and biochemical evidence that GX15-070 induces necroptosis by promoting the assembly of the necrosome on autophagosomal membranes. By linking autophagy induction to necroptosis signaling, these findings provide new insights into the mechanisms of GX15-070-induced non-apoptotic cell death.

Our findings indicating that knockdown of either Atg5 or Atg7 severely impairs the GX15-070-induced formation of autophagosomal membranes are consistent with the requirement of these two autophagy genes for vesicle elongation and formation of autophagosomes.[14] Importantly, we demonstrate genetic evidence that autophagy represents a cell death rather than a survival mechanism upon treatment with GX15-070, as blockade of autophagy by silencing either Atg5 or Atg7 severely impairs GX15-070-triggered cytotoxicity.

GX15-070 has previously been described to induce autophagy in an Atg5-[9,11] or Atg7-dependent manner.[17] However, the question whether or not autophagy represents a cell death or survival mechanism during GX15-070-mediated cytotoxicity has been controversially discussed. Although Atg5 was shown to be required for GX15-070-triggered cell death in some reports, thereby supporting a cytodestructive function of autophagy,[9,11] Atg7 knockdown failed to protect against GX15-070-induced loss of clonogenicity or ultrastructural changes in another study.[17] Also, pharmacological inhibition of autophagy using the PI3K inhibitor 3-MA was described to either inhibit[10] or enhance GX15-070-induced cell death.[18] Together, these reports suggest that GX15-070 may trigger cell death via autophagy in a context-dependent manner.

Although autophagy is predominately known for its ability to maintain cell viability, it is increasingly appreciated that autophagy can exert dual functions, acting either as a survival or cell death mechanism.[16,34] The pro-survival function of autophagy has been linked to its ability to suppress apoptosis as well as non-apoptotic forms of cell death, including necroptosis.[34–37] Vice versa, there are a number of studies showing that autophagy leads to cell death via apoptotic or non-apoptotic routes.[16,38]

On mechanistic grounds, components of autophagosomal membranes have been linked to cell death signaling pathways, in particular to apoptosis. Using the yeast two-hybrid screening system, Atg5 was found to interact with the death domain of FADD, although Atg5 itself does not contain a bona fide death domain.[39] In this model of autophagic cell death following stimulation with IFNγ, autophagy was shown to occur upstream of caspase activation, as the wide-spectrum caspase inhibitor zVAD blocked cell death but not autophagic vacuole formation.[39]

Furthermore, preautophagosomal membranes containing Atg5-Atg12-Atg16L have been shown to recruit FADD and caspase-8 to form a cytosolic complex that promotes dimerization and activation of caspase-8 in proliferating T cells.[40] In this model, caspase-8 activation was reported to support the survival of proliferating T cells by cleaving RIP1, thereby shutting down necroptosis,[40] as RIP1-dependent necroptosis was unleashed in caspase-8- or FADD-deficient T cells, where this caspase-8-mediated negative control of necroptosis was missing.[40] Interestingly, an asymmetric distribution of Atg5-Atg12-Atg16L on the outer surface of the autophagosomal isolation membrane has been reported,[15] which could facilitate the interaction of Atg5-Atg12-Atg16L with cell death signaling proteins in the cytosol.

Moreover, the sphingosine kinase inhibitor SPI-I and the proteasome inhibitor Bortezomib were described to promote self-association of caspase-8 and its autocatalytic processing on autophagosomal membranes in a Atg5- and p62-dependent manner.[41] In addition, the proteasome inhibitor MG132 has been shown to trigger oligomerization and activation of caspase-8 at intracellular membranes via the interaction of ubiquitinated caspase-8 with p62.[42] p62 is an autophagy receptor protein that binds on one side via its UBA domain to ubiquitin-tagged proteins and on the other side via its LIR domain to the autophagosomal membrane protein LC3-II.[43] As p62 was shown to bind to ubiquitinated caspase-8 to facilitate its oligomerization and activation in the cytosol,[44] p62 may serve as an additional link besides Atg5 between autophagosomal membranes and components of the apoptotic machinery. It is interesting to note that we did not detect caspase-8 recruitment to autophagosomal membranes upon treatment with GX15-070 despite expression of caspase-8 in RMS cells, suggesting that the interaction of caspase-8 with autophagosomes is regulated by additional factors.

In this context of autophagic, non-apoptotic cell death, our study is the first to show in the course of GX15-070-induced cell death that autophagy is linked to necroptosis signaling via the recruitment of the necrosome to autophagosomes. In addition, we demonstrate for the first time that RIP3 in addition to RIP1 is critically required for GX15-070-induced necroptosis. RIP1, but not RIP3, has previously been implicated in GX15-070-induced cell death in ALL cells,[10] although the underlying molecular events have so far remained elusive. Thus, together with previous reports, our findings support a model that autophagosomal membranes can engage cell death pathways via either the apoptotic or the necroptotic route, probably in a context-dependent manner. The decision which cell death program is engaged for the execution phase is likely controlled by several factors, for example, the availability and/or function of signaling proteins (e.g., caspase-8, FADD, RIP1, RIP3), the cell death stimulus or the cell type. Also, post-translational modifications may be involved, as intracellular aggregation of caspase-8 and its interaction with p62 has recently been correlated with its ubiquitination status.[42,44]

Our study has several important implications. First, we identify a molecular mechanism for GX15-070-induced non-apoptotic cell death by demonstrating that GX15-070 triggers necroptosis by promoting the assembly of the necrosome on autophagosomes. Beyond GX15-070, these findings provide, in a more general sense, new insights into the regulatory mechanisms of cell death by autophagy. A better understanding of the events that link autophagic signaling to cell death induction is especially important in order to exploit the autophagic machinery for cancer therapy.

In addition to these insights into the signal transduction pathways that are regulated by GX15-070 in cancer cells, our findings are relevant for the design of experimental therapies for RMS that aim at overcoming treatment resistance. As apoptosis is frequently impaired in RMS, for example, by overexpression of antiapoptotic Bcl-2 family proteins,[28] the activation of non-apoptotic cell death programs becomes more and more important as an alternative strategy, especially in apoptosis-resistant tumors. Thus, therapeutic induction of necroptosis may open new perspectives for the development of novel treatment approaches in cancers, including RMS.

Materials and Methods

Cell culture and chemicals. RMS cell lines were obtained from the American Type Culture Collection (Manassas, VA, USA) and maintained in RPMI 1640 (Life Technologies, Darmstadt, Germany), supplemented with 10% fetal calf serum (Biochrom, Berlin, Germany), 1 mM glutamine (Invitrogen, Karlsruhe, Germany), 1% penicillin/streptomycin (Invitrogen) and 25 mM HEPES (Biochrom). Enbrel was kindly provided by Pfizer (Berlin, Germany). zVAD.fmk was purchased from Bachem (Heidelberg, Germany), recombinant human TNFα from Biochrom, Nec-1 from Biomol (Hamburg, Germany) and all chemicals from Sigma (Deisenhofen, Germany) unless indicated otherwise.

RNA interference. For stable gene knockdown, lentiviral shRNA vectors targeting RIP1 sequence (5′-ccactagtctgacggataa-3′) or a control sequence with no corresponding part in the human genome (5′-gatcatgtagatacgctca-3′) were used as previously described.[45] Stable cell lines were produced by selection with 1 μg/ml puromycin (Sigma). For Atg5 and RIP3 knockdown, HEK293T producer cells were transfected with 7.5 μg pGIPZ-shRNAmir vector, 12.5 μg pCMV-dR8.91 and 1 μg pMD2.G using calcium phosphate transfection. All pGIPZ-shRNAmir-vectors were purchased from Thermo Fisher Scientific (Waltham, MA, USA): non-silencing control (shCtrl): RHS4346, shAtg5#1: 5′-TGAAAGAAGCTGATGCTTT-3′, shAtg5#2: 5′-GCTATATCAGGATGAGATA-3′, shRIP3#1: 5′-ACAACTACTTGAC-TATGCA-3′, and shRIP3#2: 5′-CAGAACTGTTTGTT AACGT-3′. The virus containing supernatant was collected after 48 h and filtered using a 45 μm filter. Cells were transduced by centrifugation at 1000 $\times$ *g* for 1 h at room temperature in the presence of 8 μg/ml polybrene and selected with 1 μg/ml puromycin. For transient knockdown of Atg7, cells were seeded at 1×10^5/well in a six-well tissue culture plate and allowed to settle overnight. Cells were transfected with 150 pmol of each sequence of StealthTM RNAi (Invitrogen) against Atg7 (ATG7HSS116183) or non-targeting control siRNA (12935) (Invitrogen) using TransMessenger transfection (Qiagen, Hilden, Germany), which was replaced by complete medium after 3.5 h. Seventy-two hours after transfection, cells were reseeded in a 24-well tissue culture plate, allowed to settle overnight and treated with GX15-070. For transient knockdown of TNFR1 or Bcl-2, transfection mix was prepared by diluting 20 μM of each sequence of Silencer Select (Life Technologies) non-targeting control siRNA (4390843), Bcl-2 siRNA (s14265 and s14266) or TNFR1 siRNA (s1916 and s194310) in Opti-MEM (Life Technologies) and Lipofectamine RNAiMAX Transfection Reagent (Life Technologies) and incubated for 5 min. In all, 1.5×10^5/ml cells were seeded on top of transfection medium, allowed to settle overnight and treated with GX15-070.

Determination of apoptosis, cell viability and colony formation. Apoptosis was determined by fluorescence-activated cell-sorting (FACSCanto II, BD Biosciences, Heidelberg, Germany) analysis of DNA fragmentation of propidium iodide-stained nuclei as described previously.[46] Cell viability was assessed by 3-(4,5-dimethylthiazol-2-yl)-2,5-diphenyltetrazolium bromide (MTT) assay according to the manufacturer's instructions (Roche Diagnostics, Mannheim, Germany). For colony assay, cells were seeded as single cells (100 cells/well) in six-well plates for 24 h, treated for 48 h before medium was exchanged by fresh, drug-free medium and cells were cultured for additional 10 days before staining with crystal violet solution (0.75% crystal violet, 50% ethanol, 0.25% NaCl, 1.57% formaldehyde).

Western blot analysis. Western blot analysis was performed as described previously[46] using the following antibodies: mouse anti-caspase-8 (Enzo, Lörrach, Germany), mouse anti-Bcl-2, rabbit anti-Bcl-X_L, mouse anti-Bax, mouse anti-Bak, mouse anti-RIP1, mouse anti-FADD (BD Transduction Laboratories, Heidelberg, Germany), rabbit anti-Atg5, rabbit anti-Bid, rabbit anti-Bim, rabbit anti-caspase-3, mouse anti-caspase-9 (Cell Signaling, Beverly, MA, USA), rabbit anti-Atg7 (AbCam, Cambridge, UK), rabbit anti-LC3 (Thermo Fisher Scientific Inc., Rockford, IL, USA), mouse anti-Noxa (Alexis, Grünberg, Germany), rabbit anti-Mcl-1 (Stressgen, Aachen, Germany), mouse anti-Bcl-2 (Invitrogen), mouse anti-TNFR1 (Santa Cruz Biotechnology, Santa Cruz, CA, USA) and rabbit anti-RIP3 (Imgenex, San Diego, CA, USA). Mouse anti-GAPDH (HyTest, Turku, Finland) or mouse anti-β-actin (Sigma) were used as loading controls. Goat anti-mouse IgG,

donkey anti-goat IgG, goat anti-rabbit IgG conjugated to horseradish peroxidase (Santa Cruz Biotechnology) and goat anti-mouse IgG1 or goat anti-mouse IgG2b (Southern Biotech, Birmingham, AL, USA) conjugated to horseradish peroxidase were used as secondary antibodies. Enhanced chemiluminescence (Amersham Bioscience, Freiburg, Germany) or Odyssey Infrared Imaging System (LI-COR Biosciences GmbH, Bad Homburg, Germany) were used for detection. Representative blots of at least two independent experiments are shown.

Immunoprecipitation. Immunoprecipitation of RIP1 was performed according to a previously described protocol.[45] Briefly, cells were lysed in NP40 buffer (10 mM Tris (pH 8.0), 150 mM NaCl, 1% Nonidet P-40, supplemented with a protease inhibitor tablet (Roche, Grenzach, Germany). One milligram of protein was incubated with 10 μg mouse anti-RIP1 antibody (BD Transduction Laboratories) overnight at 4 °C followed by incubation with 20 μl pan-mouse IgG Dynabeads (Invitrogen) for 2 h at 4 °C and washed with NP40 buffer. Immunoprecipitates were boiled in sample buffer for 5 min. For immunoprecipitation of FADD, cells were lysed in a buffer composed of 50 mM Tris–HCl (pH 7.5), 150 mM NaCl, 0.5% Triton X-100 and 1 mM EDTA supplemented with a protease inhibitor tablet (Roche). One milligram of protein was incubated with 10 μg with anti-FADD antibody (BD Biosciences) overnight at 4 °C followed by incubation with 20 μl pan-mouse IgG Dynabeads (Invitrogen) for 2 h at 4 °C and and washed with lysis buffer. Immunoprecipitates were boiled in sample buffer for 5 min.

Confocal microscopy. Cells were seeded in chamber slides (BD Biosciences) for 24 h before treatment, fixed with paraformaldehyde after treatment and subsequently analyzed using a Nikon C1si confocal microscope (Nikon, Tokyo, Japan).

CAM assay. CAM assay was done as described previously.[32,33] Briefly, 1×10^6 cells were implanted on fertilized chicken eggs on day 8 of incubation, treated with 100 μM GX15-070 for 4 days, sampled with the surrounding CAM, fixed in 4% paraformaldehyde, paraffin embedded, cut in 5-μm sections and were analyzed by immunohistochemistry using 1 : 1 hematoxyline and 0.5% eosin. Images were digitally recorded with an AX70 microscope (Olympus, Center Valley, PA, USA) and tumor areas were analyzed with ImageJ digital imaging software (NIH, Bethesda, MA, USA).

Statistical analysis. Statistical significance was assessed by Student's *t*-test (two-tailed distribution, two-sample, unequal variance).

Conflict of Interest

The authors declare no conflict of interest.

Acknowledgements. We thank D. Brücher for expert technical assistance, C. Hugenberg for expert secretarial assistance and Dr. J. Cinatl for help with microscopy. This work has been partially supported by grants from the Bundesministerium für Forschung und Technologie (01GM1104C) and the Deutsche Krebshilfe (to SF).

1. Lockshin RA, Zakeri Z. Cell death in health and disease. *J Cell Mol Med* 2007; **11**: 1214–1224.
2. Galluzzi L, Vitale I, Abrams JM, Alnemri ES, Baehrecke EH, Blagosklonny MV *et al.* Molecular definitions of cell death subroutines: recommendations of the Nomenclature Committee on Cell Death 2012. *Cell Death Differ* 2012; **19**: 107–120.
3. Hanahan D, Weinberg RA. Hallmarks of cancer: the next generation. *Cell* 2011; **144**: 646–674.
4. Adams JM, Cory S. The Bcl-2 apoptotic switch in cancer development and therapy. *Oncogene* 2007; **26**: 1324–1337.
5. Fulda S, Galluzzi L, Kroemer G. Targeting mitochondria for cancer therapy. *Nat Rev Drug Discov* 2010; **9**: 447–464.
6. Schimmer AD, O'Brien S, Kantarjian H, Brandwein J, Cheson BD, Minden MD *et al.* A phase I study of the pan bcl-2 family inhibitor obatoclax mesylate in patients with advanced hematologic malignancies. *Clin Cancer Res* 2008; **14**: 8295–8301.
7. Nguyen M, Marcellus RC, Roulston A, Watson M, Serfass L, Murthy Madiraju SR *et al.* Small molecule obatoclax (GX15-070) antagonizes MCL-1 and overcomes MCL-1-mediated resistance to apoptosis. *Proc Natl Acad Sci USA* 2007; **104**: 19512–19517.
8. Konopleva M, Watt J, Contractor R, Tsao T, Harris D, Estrov Z *et al.* Mechanisms of antileukemic activity of the novel Bcl-2 homology domain-3 mimetic GX15-070 (obatoclax). *Cancer Res* 2008; **68**: 3413–3420.
9. Heidari N, Hicks MA, Harada H. GX15-070 (obatoclax) overcomes glucocorticoid resistance in acute lymphoblastic leukemia through induction of apoptosis and autophagy. *Cell Death Dis* 2010; **1**: e76.
10. Bonapace L, Bornhauser BC, Schmitz M, Cario G, Ziegler U, Niggli FK *et al.* Induction of autophagy-dependent necroptosis is required for childhood acute lymphoblastic leukemia cells to overcome glucocorticoid resistance. *J Clin Invest* 2010; **120**: 1310–1323.
11. Martin AP, Mitchell C, Rahmani M, Nephew KP, Grant S, Dent P. Inhibition of MCL-1 enhances lapatinib toxicity and overcomes lapatinib resistance via BAK-dependent autophagy. *Cancer Biol Ther* 2009; **8**: 2084–2096.
12. Martin AP, Park MA, Mitchell C, Walker T, Rahmani M, Thorburn A *et al.* BCL-2 family inhibitors enhance histone deacetylase inhibitor and sorafenib lethality via autophagy and overcome blockade of the extrinsic pathway to facilitate killing. *Mol Pharmacol* 2009; **76**: 327–341.
13. Wei Y, Kadia T, Tong W, Zhang M, Jia Y, Yang H *et al.* The combination of a histone deacetylase inhibitor with the Bcl-2 homology domain-3 mimetic GX15-070 has synergistic antileukemia activity by activating both apoptosis and autophagy. *Clin Cancer Res* 2010; **16**: 3923–3932.
14. Nakatogawa H, Suzuki K, Kamada Y, Ohsumi Y. Dynamics and diversity in autophagy mechanisms: lessons from yeast. *Nat Rev Mol Cell Biol* 2009; **10**: 458–467.
15. Mizushima N, Yoshimori T, Ohsumi Y. The role of Atg proteins in autophagosome formation. *Annu Rev Cell Dev Biol* 2011; **27**: 107–132.
16. Fulda S. Autophagy and cell death. *Autophagy* 2012; **8**: 1250–1251.
17. McCoy F, Hurwitz J, McTavish N, Paul I, Barnes C, O'Hagan B *et al.* Obatoclax induces Atg7-dependent autophagy independent of beclin-1 and BAX/BAK. *Cell Death Dis* 2010; **1**: e108.
18. Pan J, Cheng C, Verstovsek S, Chen Q, Jin Y, Cao Q. The BH3-mimetic GX15-070 induces autophagy, potentiates the cytotoxicity of carboplatin and 5-fluorouracil in esophageal carcinoma cells. *Cancer Lett* 2010; **293**: 167–174.
19. Wei CC, Ball S, Lin L, Liu A, Fuchs JR, Li PK *et al.* Two small molecule compounds, LLL12 and FLLL32, exhibit potent inhibitory activity on STAT3 in human rhabdomyosarcoma cells. *Int J Oncol* 2011; **38**: 279–285.
20. Vandenabeele P, Declercq W, Van Herreweghe F, Vanden Berghe T. The role of the kinases RIP1 and RIP3 in TNF-induced necrosis. *Sci Signal* 2010; **3**: re4.
21. Hitomi J, Christofferson DE, Ng A, Yao J, Degterev A, Xavier RJ *et al.* Identification of a molecular signaling network that regulates a cellular necrotic cell death pathway. *Cell* 2008; **135**: 1311–1323.
22. He S, Wang L, Miao L, Wang T, Du F, Zhao L *et al.* Receptor interacting protein kinase-3 determines cellular necrotic response to TNF-alpha. *Cell* 2009; **137**: 1100–1111.
23. Vandenabeele P, Galluzzi L, Vanden Berghe T, Kroemer G. Molecular mechanisms of necroptosis: an ordered cellular explosion. *Nat Rev Mol Cell Biol* 2010; **11**: 700–714.
24. Dagher R, Helman L. Rhabdomyosarcoma: an overview. *Oncologist* 1999; **4**: 34–44.
25. Merlino G, Helman LJ. Rhabdomyosarcoma—working out the pathways. *Oncogene* 1999; **18**: 5340–5348.
26. Margue CM, Bernasconi M, Barr FG, Schafer BW. Transcriptional modulation of the anti-apoptotic protein BCL-XL by the paired box transcription factors PAX3 and PAX3/FKHR. *Oncogene* 2000; **19**: 2921–2929.
27. Pazzaglia L, Chiechi A, Conti A, Gamberi G, Magagnoli G, Novello C *et al.* Genetic and molecular alterations in rhabdomyosarcoma: mRNA overexpression of MCL1 and MAP2K4 genes. *Histol Histopathol* 2009; **24**: 61–67.
28. Fulda S. Cell death pathways as therapeutic targets in rhabdomyosarcoma. *Sarcoma* 2012; **2012**: 326210.
29. Hayes-Jordan A, Andrassy R. Rhabdomyosarcoma in children. *Curr Opin Pediatr* 2009; **21**: 373–378.
30. Klionsky DJ. The autophagosome is overrated! *Autophagy* 2011; **7**: 353–354.
31. Degterev A, Huang Z, Boyce M, Li Y, Jagtap P, Mizushima N *et al.* Chemical inhibitor of nonapoptotic cell death with therapeutic potential for ischemic brain injury. *Nat Chem Biol* 2005; **1**: 112–119.
32. Stupack DG, Teitz T, Potter MD, Mikolon D, Houghton PJ, Kidd VJ *et al.* Potentiation of neuroblastoma metastasis by loss of caspase-8. *Nature* 2006; **439**: 95–99.
33. Hacker S, Dittrich A, Mohr A, Schweitzer T, Rutkowski S, Krauss J *et al.* Histone deacetylase inhibitors cooperate with IFN-gamma to restore caspase-8 expression and overcome TRAIL resistance in cancers with silencing of caspase-8. *Oncogene* 2009; **28**: 3097–3110.
34. Gump JM, Thorburn A. Autophagy and apoptosis: what is the connection? *Trends Cell Biol* 2011; **21**: 387–392.
35. Shen HM, Codogno P. Autophagy is a survival force via suppression of necrotic cell death. *Exp Cell Res* 2012; **318**: 1304–1308.
36. Wu YT, Tan HL, Huang Q, Ong CN, Shen HM. Activation of the PI3K-Akt-mTOR signaling pathway promotes necrotic cell death via suppression of autophagy. *Autophagy* 2009; **5**: 824–834.
37. Wu YT, Tan HL, Huang Q, Kim YS, Pan N, Ong WY *et al.* Autophagy plays a protective role during zVAD-induced necrotic cell death. *Autophagy* 2008; **4**: 457–466.

38. Yu L, Alva A, Su H, Dutt P, Freundt E, Welsh S *et al.* Regulation of an ATG7-beclin 1 program of autophagic cell death by caspase-8. *Science* 2004; **304**: 1500–1502.
39. Pyo JO, Jang MH, Kwon YK, Lee HJ, Jun JI, Woo HN *et al.* Essential roles of Atg5 and FADD in autophagic cell death: dissection of autophagic cell death into vacuole formation and cell death. *J Biol Chem* 2005; **280**: 20722–20729.
40. Bell BD, Leverrier S, Weist BM, Newton RH, Arechiga AF, Luhrs KA *et al.* FADD and caspase-8 control the outcome of autophagic signaling in proliferating T cells. *Proc Natl Acad Sci USA* 2008; **105**: 16677–16682.
41. Young MM, Takahashi Y, Khan O, Park S, Hori T, Yun J *et al.* Autophagosomal membrane serves as platform for intracellular death-inducing signaling complex (iDISC)-mediated caspase-8 activation and apoptosis. *J Biol Chem* 2012; **287**: 12455–12468.
42. Pan JA, Ullman E, Dou Z, Zong WX. Inhibition of protein degradation induces apoptosis through a microtubule-associated protein 1 light chain 3-mediated activation of caspase-8 at intracellular membranes. *Mol Cell Biol* 2011; **31**: 3158–3170.
43. Behrends C, Fulda S. Receptor proteins in selective autophagy. *Int J Cell Biol* 2012; **2012**: 673290.
44. Jin Z, Li Y, Pitti R, Lawrence D, Pham VC, Lill JR *et al.* Cullin3-based polyubiquitination and p62-dependent aggregation of caspase-8 mediate extrinsic apoptosis signaling. *Cell* 2009; **137**: 721–735.
45. Loeder S, Schirmer M, Schoeneberger H, Cristofanon S, Leibacher J, Vanlangenakker N *et al.* RIP1 is required for IAP inhibitor-mediated sensitization of childhood acute leukemia cells to chemotherapy-induced apoptosis. *Leukemia* 2012; **26**: 1742.
46. Fulda S, Sieverts H, Friesen C, Herr I, Debatin KM. The CD95 (APO-1/Fas) system mediates drug-induced apoptosis in neuroblastoma cells. *Cancer Res* 1997; **57**: 3823–3829.

Supplementary Information accompanies this paper on Cell Death and Differentiation website (http://www.nature.com/cdd)